Volume 1
Number 4
August 2022
Pages 347-542

Digital Discovery

rsc.li/digitaldiscovery

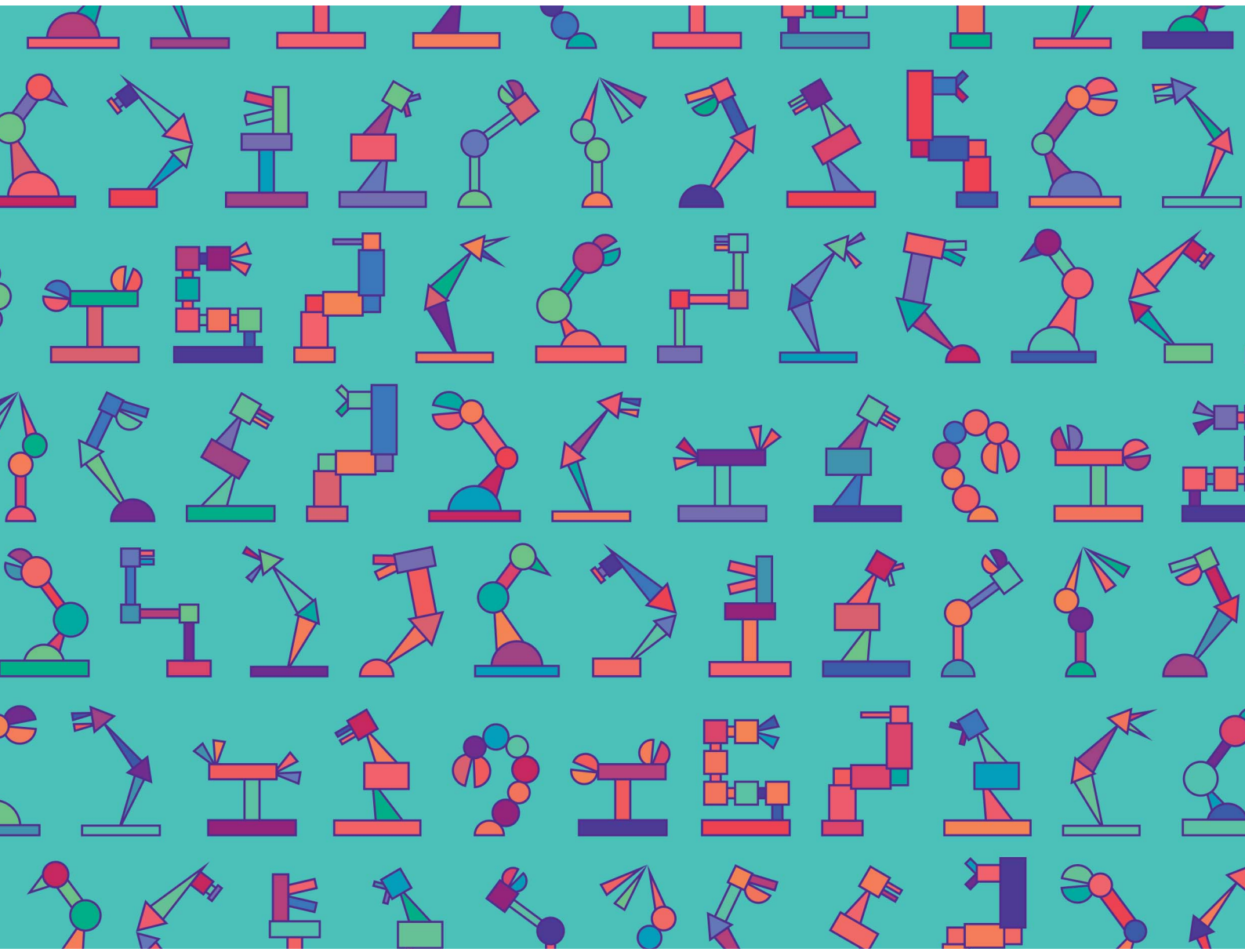

ISSN 2635-098X

ROYAL SOCIETY OF CHEMISTRY

PAPER
Curtis P. Berlinguette *et al.*
A self-driving laboratory designed to accelerate the discovery of adhesive materials

Digital Discovery

ROYAL SOCIETY OF CHEMISTRY

PAPER

View Article Online
View Journal | View Issue

Cite this: *Digital Discovery*, 2022, **1**, 382

A self-driving laboratory designed to accelerate the discovery of adhesive materials†

Michael B. Rooney, ‡[a] Benjamin P. MacLeod, ‡[ab] Ryan Oldford, [a] Zachary J. Thompson,[e] Kolby L. White,[e] Justin Tungjunyatham,[e] Brian J. Stankiewicz [e] and Curtis P. Berlinguette *[abcd]

Received 4th April 2022
Accepted 28th May 2022

DOI: 10.1039/d2dd00029f

rsc.li/digitaldiscovery

We report a self-driving laboratory for adhesive material optimization. This autonomous laboratory combines a robot for preparing and testing adhesive bonds with a Bayesian optimizer to rapidly improve adhesive formulations. This system uses a single robot to perform a complex sequence of eight tasks including surface preparation, test specimen assembly, and bond strength evaluation. To enable automated strength testing, we developed an automated pull test method that correlates linearly with a single-lap-joint shear test method. This work demonstrates how flexible automation accelerates complex, multi-step experimental workflows for which commercial automation solutions are not available.

Introduction

Adhesives are an easy to use, inexpensive way to bond materials together.[1] A wide range of ingredients are used to customize adhesives for different applications.[1–4] Optimized adhesive formulations may contain six or more components (Fig. 1). It is extremely difficult to predict the properties of the resulting disordered composites *a priori*.[5] This challenge is compounded by the fact that bond strength depends not only on the chemical makeup of the adhesive, but also on the properties of the adhesive/adherend interfaces.[1] These challenges make the discovery of new adhesives highly empirical.

New adhesives are developed by iteratively preparing and testing experimental formulations. The overall adhesive development process is time-consuming because the number of possible formulations is large and multiple test specimens must be made and broken to characterize each formulation. One of the most common adhesive characterization methods is the single-lap-joint shear test ("lap shear" – *e.g.* ASTM D1002 [6]), where the test specimen consists of two rectangular coupons of material bonded together in an overlapping geometry (Fig. 1). The shear stress required to separate these coupons is a measure of the adhesive bond strength.[6] The preparation of reliable and reproducible lap shear specimens requires a researcher to manually clean and abrade the coupons, deposit adhesive on them, close the joints, and fixture them in place for curing. The researcher must then wait hours to days for the specimens to cure before testing them. This testing is typically done by manually loading specimens into a universal tester one at a time. Although autosampling universal testers exist,[7] they do not eliminate the time-consuming manual preparation of test specimens. This specimen preparation bottleneck limits the rate at which new formulations can be tested. The cognitive challenge of optimizing a multi-component formulation also slows the development of new adhesives. Here we describe a self-driving robotic laboratory which addresses both the rate of adhesive specimen testing and the challenge of choosing which formulations to test.

Our self-driving laboratory uses a robot to automatically create and test adhesive specimens. This robot employs a dolly pull-off test,[8–10] which we show correlates with manual lap shear tests. The robot operator is only responsible for the initial stocking of consumables and dispensing the adhesive. Once set up, the laboratory can run without direct supervision and test up to 50 independent samples before restocking. Our robot significantly reduces the existing manual labor requirement of specimen creation and offers precise control over the time between forming and testing the bond.

We combined this robot with a Bayesian optimizer to enable the autonomous optimization of an adhesive formulation (Fig. 2). Bayesian optimizers iteratively search for input parameters that maximize an outcome and have previously been used to guide manual optimization of adhesive formulations.[11] Autonomous workflows that combine optimizers with

[a]*Department of Chemistry, The University of British Columbia, 2036 Main Mall, Vancouver, British Columbia, Canada, V6T 1Z1. E-mail: cberling@chem.ubc.ca*

[b]*Stewart Blusson Quantum Matter Institute, The University of British Columbia, 2355 East Mall, Vancouver, British Columbia, Canada, V6T 1Z4*

[c]*Department of Chemical & Biological Engineering, The University of British Columbia, 2360 East Mall, Vancouver, British Columbia, Canada, V6T 1Z3*

[d]*Canadian Institute for Advanced Research (CIFAR), MaRS Innovation Centre, 661 University Ave. Suite 505, Toronto, Ontario, Canada, M5G 1M1*

[e]*3M Company, 3M Center, Maplewood, Minnesota 55144, USA*

† Electronic supplementary information (ESI) available. See https://doi.org/10.1039/d2dd00029f

‡ These authors contributed equally to this work.

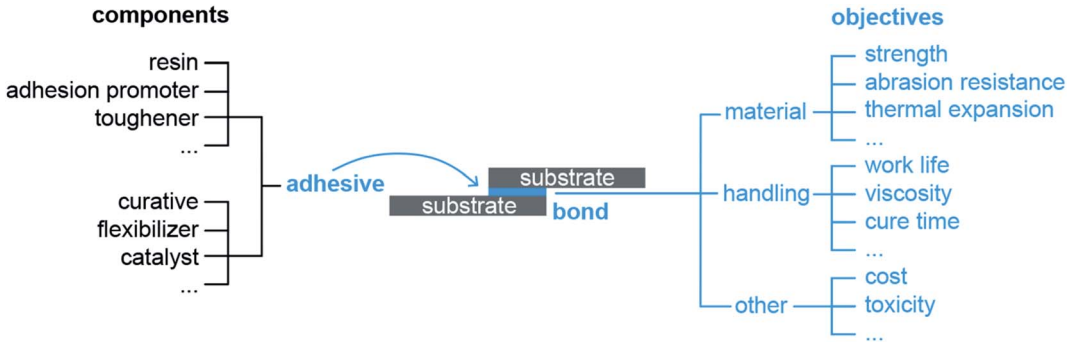

Fig. 1 Adhesives are complex, multi-component materials which must satisfy multiple objectives. Two-part formulations may include six or more components. An adhesive must satisfy several objectives depending on the application. The fully cured material must exhibit suitable physical properties while the uncured material must have appropriate handling characteristics. Other important objectives include cost and toxicity. A single-lap-joint shear test specimen is shown in the middle; it is composed of two flat substrates bonded by an adhesive of known area.

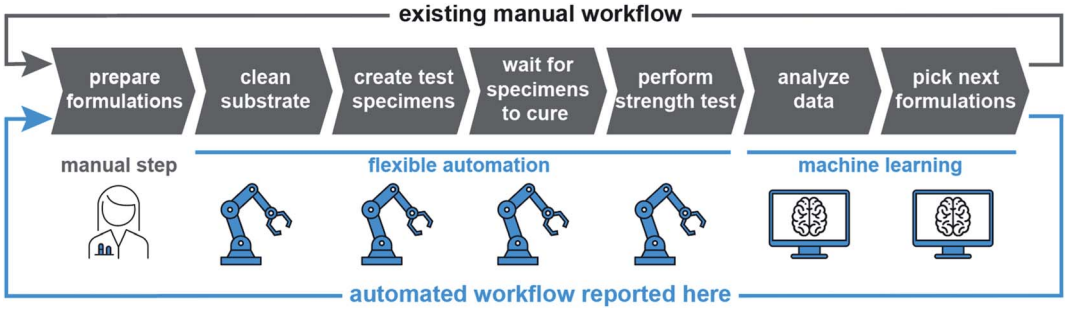

Fig. 2 A workflow for optimizing the strength of an adhesive formulation. This workflow involves preparing adhesive formulations, cleaning substrates using abrasives and solvents, and then using these formulations and substrates to create test specimens. The test specimens are then cured, and their strength is measured. The data is analyzed, and the results are used to design improved formulations for the next round of experiments. Typically, all the steps of this lengthy procedure are performed manually. Here we automated six of the seven steps using flexible automation and machine learning.

robotic experiments to optimize formulations are nascent[12,13] and have not yet been reported for adhesives research. To demonstrate the capabilities of our self-driving laboratory, we used it to maximize the bond strength of a two-part epoxy by optimizing the resin to hardener ratio.

Experimental

The preparation of overlap shear test specimens is difficult to automate. We therefore devised an alternate bond strength testing method more amenable to automation (Fig. 3). Specifically, we adapted a standard pull-off testing method (normally used to measure coating adhesion[14]) to enable the automated testing of adhesive strength. This pull-off method involves adhering an aluminum dolly to a substrate, pulling off the dolly using a force normal to the substrate with a commercially available testing head, and recording the maximum force required to break the bond (Fig. 3a and j). We built on our previous self-driving laboratories,[15,16] by constructing the system described here using a 4-axis robotic arm (N9, North Robotics) (Fig. 4 and S1†). We leveraged rapid prototyping to develop the custom hardware components necessary for the flexible automated workflow executed by this robot. The robotic system was controlled through a custom graphical user interface (UI) built in Python (Fig. S3†). The steps in the robotic workflow (preparation, adherend cleaning, specimen assembly and curing, bond strength measurement, see Fig. 3 and Video S1†) are described in more detail below.

To prepare the robotic platform for operation, it was first manually stocked with dollies and test plates. The software was then configured to run the desired test. The workflow presented here used commercially available aluminum dollies with 10 mm or 20 mm diameter bond areas (Defelsko Corporation). Up to 50 dollies could be placed within reach of the robot on two dolly trays (25 dollies each). Test plates were waterjet cut from $\frac{1}{4}$ inch-thick 6061 aluminum sheets. Two alignment holes in each test plate facilitated accurate fixturing on the robotic platform. Other consumable items requiring periodic restocking included: a foam brush, isopropanol bath, abrasive pad, and abrasive tool.

The first step in the workflow was the automated cleaning of both the dollies and the test plates (Fig. 3c–f). The bottom face of each dolly was abraded by rapidly rotating the dolly (using the robot arm's gripper rotation) while in contact with an abrasive pad. The dolly was dipped in an isopropyl alcohol (IPA) bath to clean away the dust generated by the abrasion step and dried in

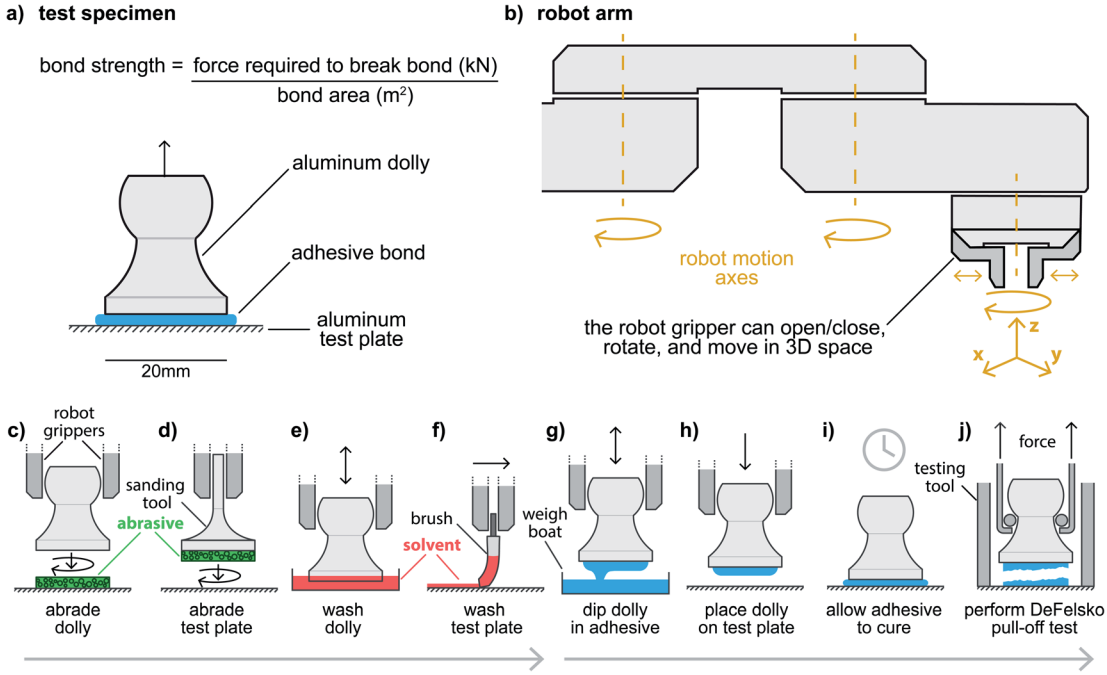

Fig. 3 Multi-step robotic workflow for adhesive specimen preparation and testing. (a) The adhesive test specimen employed in the workflow is a pull-off type consisting of an aluminum dolly adhered to an aluminum plate. (b) A 4-axis robotic arm including a rotating gripper was employed for this study. The major steps in the workflow executed by the robot are (c) and (d) abrasive cleaning of the dolly and test plate, (e) and (f) solvent cleaning of the dolly and test plate, (g) and (h) assembly of the test specimen by dipping the dolly into a weigh boat containing adhesive and then placing the dolly on the test plate, (i) curing of the adhesive under ambient conditions, and (j) strength testing by measuring the force required to break the bond between the dolly and the test plate.

a stream of compressed N_2 gas. Digital photographs of the dolly's bottom face were taken at the camera station (BFS-U3-120S4C-CS, Teledyne FLIR LLC) before and after cleaning, and saved with all workflow data. The test plates were abraded by a medium coarse rotating abrasive disk tool which was held by the robot's rotating gripper and pressed downward onto the test plate. The distance between the gripper and test plate was manually adjusted until test plates were visibly cleaned of contaminants, and a consistent surface finish was observed. The robot arm did not have force feedback, however the downward force applied by the abrasive tool to the test plate was estimated to be 20 N. Accumulated dust and abrasion particulates were brushed clean with a disposable foam brush wetted with IPA. The foam brush was automatically cleaned by sonication in an IPA bath (PC3, L & R Manufacturing), then dried with a stream of N_2 compressed gas. After cleaning both the dollies and the test plates, the robot assembled each specimen by picking up a dolly, dipping it in adhesive, and then placing it onto the test plate. Up to 25 specimens in a 5×5 pattern could be placed on each test plate. The adhesives to be tested are stored in trays adjacent to the test plates on the robotic platform. Each tray contained up to 5 adhesive formulations to test. Each formulation was stored in a disposable weigh boat and contained enough adhesive for up to 5 specimens. To set bond thickness, glass spacer beads (Envirospheres, E-SPHERES SL Grade SLG, mean particle size 0.130 mm) were manually mixed into the adhesive at 0.5% of the total adhesive mass. When the robot is ready to begin assembling specimens, the robot prompts the operator to manually dispense the adhesives to be tested into the weigh boats. For the two-part epoxies studied here (3M™ Scotch-Weld™ Epoxy Adhesive DP190 Gray and 3M™ Scotch-Weld™ Epoxy Adhesive DP420 Black), we experimentally determined that approximately 0.33 g of adhesive is needed per specimen. The robot arm dipped the dolly into the adhesive, performed pre-set movements to minimize dripping, and placed the dolly on the test plate. The robot placed each dolly on the test plate at a fixed height set to ensure the dolly firmly contacted the plate before being released by the gripper. The robotic system offers precise control over the time between bond formation and strength measurement. The bond strength measurements were performed one specimen at a time after a predetermined curing period.

The robot measured the adhesive bond strengths using a commercial pull-off adhesion tester (PosiTest ATA20, DeFelsko, Fig. 4b). This tester consists of a hydraulic actuator and a quick-release collar configured to pull a dolly away from a test plate with up to 7.55 kN of force. This tool was originally designed for manual use, so we modified it in order to automate its functions, and to enable it to be picked up by the robot (Fig. 4b and S2†). A 3D-printed chassis along with pneumatic pistons were added to the testing tool to actuate the internal collar. A longer metal handle was added to the tester tool to provide a cylindrical feature for the robot to grip. These modifications enabled fully automated docking, testing, and ejection of dollies. After locking on to a dolly, the test head increased the force at a rate of approximately 300 N s^{-1} until the bond failed.

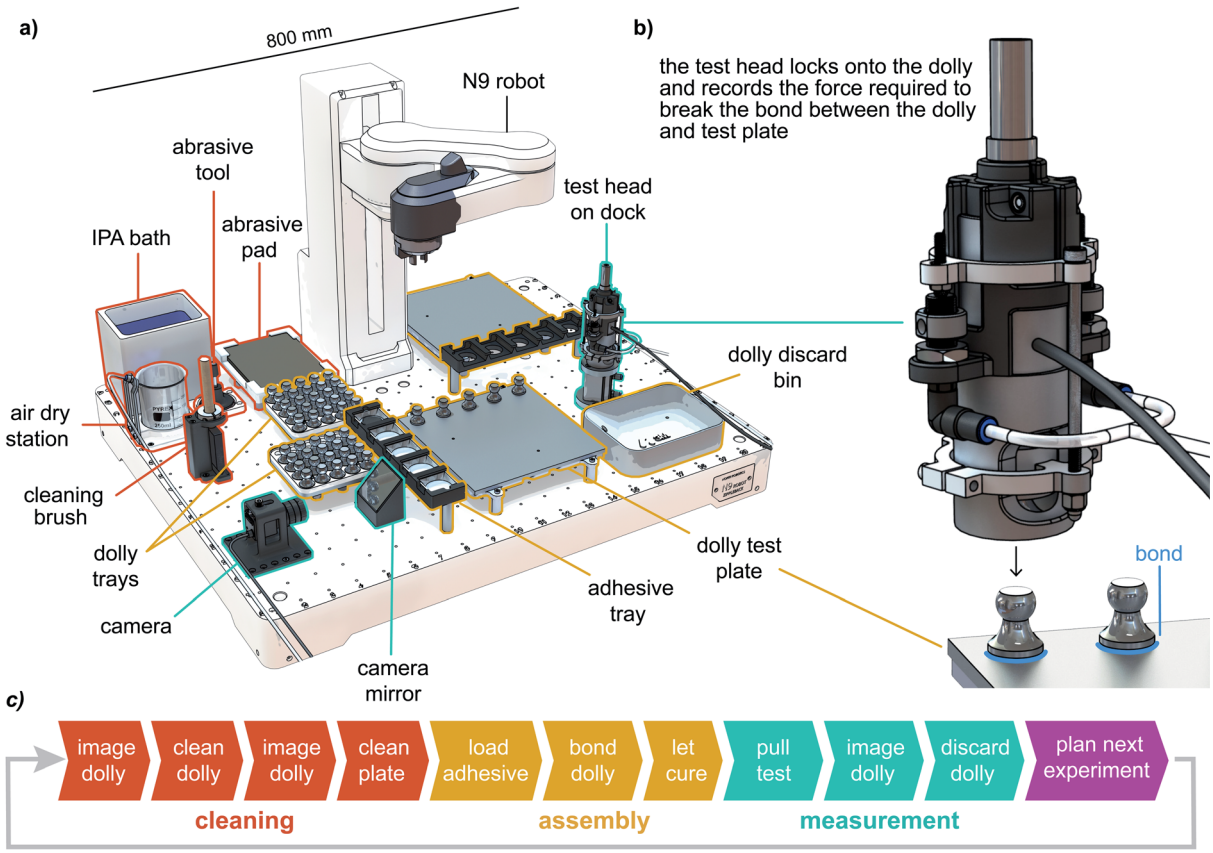

Fig. 4 Robotic platform used to automatically create and test adhesive specimens. (a) The robot, stations, and tools used to execute the automated workflow (see also Fig. S1†). This system can create up to 50 test specimens from up to 10 unique formulations before the consumables (adhesives, dollies and test plates) need to be replenished. (b) Detailed view of the hydraulic strength testing tool used by the robot to measure bond strength. A variety of custom components added to the strength testing tool to enable automated operation are shown (see also Fig. S2†). (c) The sequence of operations performed by the system. After data is obtained by the robot, a Bayesian optimization algorithm is used to design the next batch of formulations to test.

The normal force required to break the bond between the dolly and plate was recorded for each specimen. After performing the pull-off test, the robot captured an image of the adhesive failure surface on the dolly's bottom face. The robot then ejected the dolly into a discard bin, and reset the test head. This pull test took approximately 2 minutes, and was repeated for each dolly on the test plate.

Results and discussion

To assess the validity of our automated pull tests we compared them to manual lap shear tests for two commercial epoxies (3M™ Scotch-Weld™ Epoxy Adhesive DP190 Gray and 3M™ Scotch-Weld™ Epoxy Adhesive DP420 Black) at varying cure times (Fig. 5 and Tables S1–S3†). The resulting data showed a linear correlation between the automated pull test and manual lap shear methods for each epoxy.

3M™ Scotch-Weld™ Epoxy Adhesive DP190 Gray is a flexible epoxy. Flexible epoxies provide an elastic bond that enables some movement between the adherends without failure. We compared pull-off tests for this epoxy to manual lap shear tests performed in our laboratory. These lap shear tests used 4 × 1 × 0.0625 inch aluminum coupons that were prepared by sandblasting followed by wiping with isopropanol before assembly with a 0.5 inch overlap using 0.003 inch diameter glass beads to control the bond thickness. The correlation slope between the tensile stress of the pull-off test and the shear stress of the lap shear tests was 2.29 over the range of cure conditions tested. 3M™ Scotch-Weld™ Epoxy Adhesive DP420 Black is a toughened epoxy. Toughened epoxies provide a more rigid but impact and fatigue-resistant bond. We compared pull-off tests for this epoxy to manual lap shear data from the material technical data sheet.[17] The correlation slope was 0.72 (Fig. 5).

Correlations for both epoxy adhesives exhibited high degrees of linearity ($R^2 = 0.99$ for 3M™ Scotch-Weld™ Epoxy Adhesive DP190 Gray; $R^2 = 0.99$ for 3M™ Scotch-Weld™ Epoxy Adhesive DP420 Black). We attribute the differences in correlation slope to the very different mechanical properties of the two adhesives (flexible *vs.* toughened) and the different lap shear procedures employed (our manual preparation and testing of lap shear samples *vs.* datasheet reported values). These results show that the pull-off test is suitable for comparing the relative strengths of a given type of adhesive and can track rate-of-strength build as a function of cure time.

To demonstrate the capabilities of our self-driving laboratory, we used it to maximize the bond strength of an adhesive

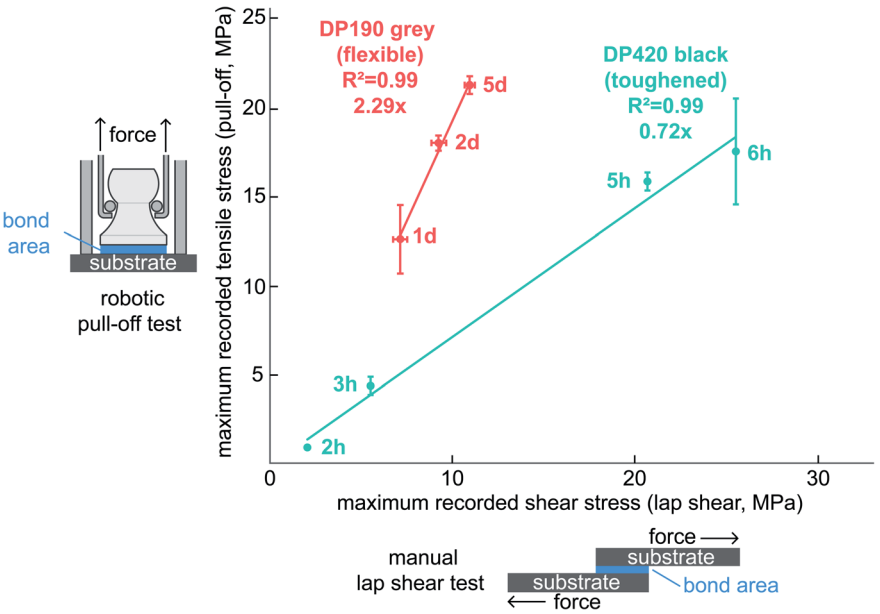

Fig. 5 Correlation between automated (pull-off) and manual (lap shear) adhesive strength tests. Bond strength data was obtained using triplicate pull-off tests executed by our robotic system, triplicate manual lap shear tests for 3M™ Scotch-Weld™ Epoxy Adhesive DP190 Gray, and referenced lap shear data for 3M™ Scotch-Weld™ Epoxy Adhesive DP420.[17] Both adhesives were tested over a range of curing conditions (2–6 hours for 3M™ Scotch-Weld™ Epoxy Adhesive DP420, 1–5 days for 3M™ Scotch-Weld™ Epoxy Adhesive DP190 Gray) to assess the adhesive strength correlation over a wider range of values. Horizontal and vertical error bars indicate standard deviations of the recorded stresses across replicate samples.

formulation. We performed this optimization by coupling our automated workflow to a Bayesian optimizer.[15,16] Bayesian optimizers combine a surrogate model with an acquisition function. The surrogate model predicts the response of an experiment to the manipulated variables. The acquisition function determines which experiment(s) should be performed next to optimize the outcome of the experiment. The Bayesian optimization performed here manipulated the ratio of resin to hardener in a two-part epoxy system to maximize the strength as measured using the robotic pull-off test. We expressed this manipulated variable as a resin fraction $R = \text{mass}_{\text{resin}}/(\text{mass}_{\text{resin}} + \text{mass}_{\text{hardner}})$ to obtain a variable ranging from 0 to 1. The resin and hardener used in the formulation were taken from a commercially available two-part epoxy (3M™ Scotch-Weld™ Epoxy Adhesive DP420 Black).

We leveraged the ability of the robotic system to test multiple formulations in parallel by employing the AX Bayesian optimization package which supports batchwise acquisition of data from the experiment using the q-noisy expected improvement (qNEI) acquisition function.[18,19] Once a batch of formulations was requested by this optimizer, formulations with the requested resin fraction were prepared by manually weighing individual components into a weigh boat on a digital weigh scale. The formulations were then mixed by hand with a stir stick before being loaded onto the robotic platform. This step was followed by completely automated specimen preparation, curing for 3 h, and testing. The resulting data is used to update the optimizer's surrogate model and a new batch of formulations is requested, beginning the next round of the optimization.

Each round of the optimization involved testing a batch of five formulations in triplicate (Fig. 6 and Tables S4–S7†). The resin fractions for the five formulations tested in the first round were selected using a scrambled sobol sequence. The resulting data was used to initialize the Gaussian process surrogate model used by the optimizer. The sobol sequence and surrogate function used the default settings implemented in the AX Bayesian optimization package.[18] The resin fractions for subsequent rounds were selected by the optimizer using the qNEI acquisition function. Dolly images acquired after the pull-off tests showed wet-looking residual material consistent with incompletely cured adhesive for resin ratios below 0.2 or above 0.7. The images of dollies with resin ratios between 0.2 and 0.7 showed dry-looking residual material consistent with cured adhesive. The region containing the optimal resin fraction to maximize strength was very clearly defined after four rounds of optimization. In the particular experimental optimization campaign shown here, the formulation with the highest strength was identified in round 1 by random chance. Simulated optimization campaigns using the same optimizer configuration as the real-world experiments showed that when the optimum formulation is not identified in round 1, the optimizer will converge on the optimal formulation in subsequent rounds (see Fig. S4†). These results demonstrate that our self-driving laboratory can find an optimal resin fraction for maximizing the tensile strength of a 2-part epoxy. This self-driving lab could be adapted to the optimization of more complex formulations.

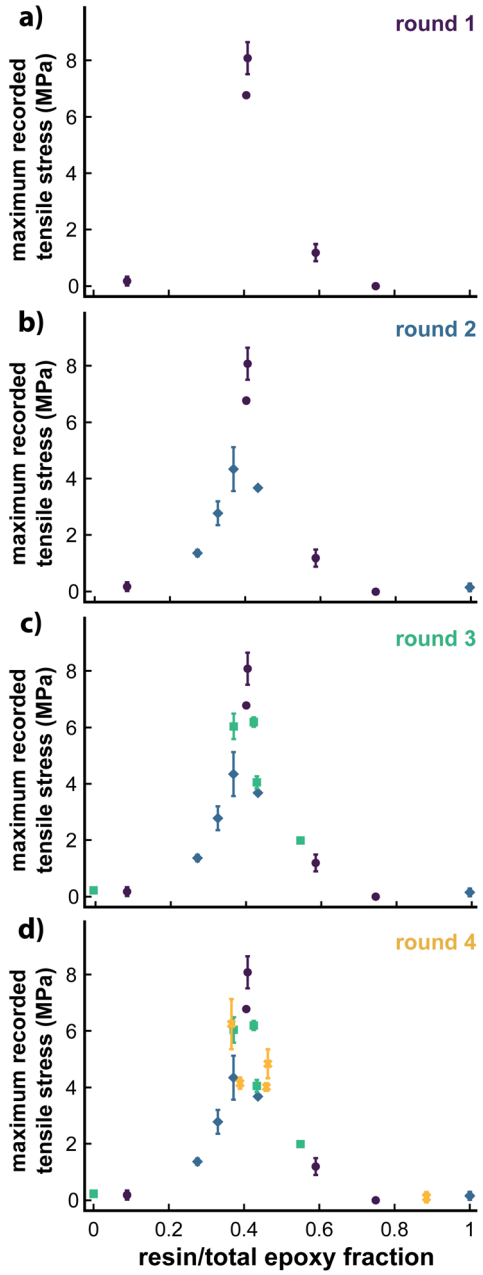

Fig. 6 Optimization of an adhesive formulation by a self-driving laboratory. In each round of the optimization, five adhesive formulations were cured for 3 h and then tested in triplicate. The mean and standard deviation of the pull-off force for each formulation are shown. In round 1 (a), the five formulations were selected using a scrambled sobol sequence. In the following rounds (b)–(d), the formulations were selected by a Bayesian optimizer configured to maximize the pull-off force of the adhesive by manipulating the ratio of base to accelerant of a commercial two-part epoxy adhesive (3M™ Scotch-Weld™ Epoxy Adhesive DP420 Black).

Conclusions

We demonstrated a self-driving laboratory that can optimize an epoxy formulation to maximize the bond strength. This system reduces human effort by automating specimen preparation and testing, and by using a Bayesian optimizer to choose which formulations to test next. The automated workflow used a single robot to perform a complex sequence of eight tasks, including a pull-off strength test. This test correlates with standard lap shear tests and is suitable for optimizing adhesive bond strength. This self-driving laboratory for adhesives could be improved in several ways.

For example, increased ambient lab temperatures in optimization round 4 increased the curing rate, resulting in increased strength at the same epoxy fraction (compare Fig. 4c with Fig. 4d). A temperature-controlled curing environment would mitigate this problem. We note that the samples in this study were cured for less time than specified in the technical datasheet.

Consistent surface preparation is critical to obtaining repeatable bond strength data. While we manually changed the abrasion tools and pads employed in our setup at regular intervals to maintain consistent surface preparation, a more advanced system might automatically use fresh abrasion media on a schedule. Alternatively, fresh adhesive media could be adaptively requested by the system in response to feedback from automated surface quality assurance measurements.

In this study, we manually developed a dip and place routine that minimized unwanted dripping of adhesives. To facilitate working with new adhesives having different fluid characteristics, automatic optimization of the dip and place routine using feedback (*e.g.*, from a weigh scale or machine vision) would be beneficial.

Our robotic system automatically photographs the bottom surface of every dolly after testing. These images could be automatically processed with machine vision to help classify the bond failure mode or categorize morphological defects.[20] This information could be used to alert the researcher if an outlier occurred.

While we presented a single-parameter, single-objective optimization here, this optimization could be extended to incorporate multiple manipulated variables or multiple optimization objectives. Such extensions would be synergistic with hardware upgrades.[12,16] For example, incorporating an oven into the robot would enable the optimization of thermal curing protocols. Expert knowledge (such as the range of resin ratios likely to yield high strength) or bond strength estimates based on simulations[21] could also be incorporated to increase the efficiency of the Bayesian optimization.[22,23]

This work shows how flexible automation can enable materials scientists to automate complex, multi-step experimental workflows for which commercial automation solutions are not available.[24] Self-driving laboratories will empower human experts to rapidly develop high performance adhesives and other complex formulated materials.

Data availability

The experimental data are provided in the ESI.† The code used for the simulations shown in Fig. S4† is available at **https://github.com/berlinguette/ada**.

Author contributions

Michael B. Rooney: conceptualization, methodology, visualization, writing – original draft preparation. Benjamin P. MacLeod: conceptualization, methodology, writing – original draft preparation. Ryan Oldford: software, methodology, visualization, writing – review & editing. Zachary J. Thompson: methodology, writing – review & editing. Kolby L. White: methodology, writing – review & editing. Justin Tungjunyatham: methodology, writing – review & editing. Brian Stankiewicz: conceptualization, methodology, funding acquisition, writing – review & editing. Curtis P. Berlinguette: conceptualization, methodology, funding acquisition, writing – review & editing.

Funding

We thank 3M Company, 3M Innovative Properties Company, and the Natural Sciences and Engineering Research Council of Canada (CRDPJ 543581-19) for their financial support. C. P. B. is grateful to the Canadian Foundation for Innovation (229288), the Canadian Institute for Advanced Research (BSE-BERL-162173), and the Canada Research Chairs Program for financial support. B. P. M. and C. P. B. acknowledge support from the SBQMI's Quantum Electronic Science and Technology Initiative, the Canada First Research Excellence Fund, and the Quantum Materials and Future Technologies Program.

Conflicts of interest

The authors declare no conflict of interest.

Acknowledgements

We gratefully acknowledge Karry Ocean, Alex Proskurin, and Caroline Krzyszkowski for engineering and research support, and Fraser Parlane for his assistance creating figures. We thank CMC Microsystems for the provision of products and services that facilitated this research, including SolidWorks 2019 SP5.0. For software that facilitated robot control and data processing, we acknowledge the contributors to the Python programming language (Python Software Foundation, https://www.python.org).

References

1 S. Ebnesajjad and A. H. Landrock, Chapter 1 – Introduction and Adhesion Theories, in *Adhesives Technology Handbook*, ed. S. Ebnesajjad and A. H. Landrock, William Andrew Publishing, Boston, 3rd edn, 2015, pp. 1–18.

2 L. T. Tseng, R. H. Jhang, J. Q. Ho and C. H. Chen, Molecular Approach to Enhance Thermal Conductivity in Electrically Conductive Adhesives, *ACS Appl. Electron. Mater.*, 2019, **1**(9), 1890–1898.

3 G. H. Shim, B. Kweon, M. S. Lee, J. H. Kim, T. S. Jun, T. Kim, *et al.*, Highly improved mechanical and thermal properties of alkali silicate and graphene nanoplatelet composite adhesives, *Int. J. Adhes. Adhes.*, 2021, **110**, 102942.

4 J. S. Kang, A. J. Myles and K. D. Harris, Thermally-Degradable Thermoset Adhesive Based on a Cellulose Nanocrystals/Epoxy Nanocomposite, *ACS Appl. Polym. Mater.*, 2020, **2**(11), 4626–4631.

5 H. Quan and R. Alderliesten, On the effect of plastic model on simulation of adhesive bonded joints with FM94, *Int. J. Adhes. Adhes.*, 2021, **110**, 102916.

6 American Society for Testing and Materials, Standard Test Method for Apparent Shear Strength of Single-Lap Joint Adhesively Bonded Metal Specimens by Tension Loading (Metal-to-Metal), ASTM, 2019, Report No.: D1002-10, available from: https://www.astm.org/d1002-10r19.html.

7 Illinois Tool Works Inc., Instron Automated Testing Systems, available from: https://www.instron.com/en-us/products/testing-systems/automated-testing-systems.

8 B. J. Chisholm, D. C. Webster, J. C. Bennett, M. Berry, D. Christianson, J. Kim, *et al.*, Combinatorial materials research applied to the development of new surface coatings VII: an automated system for adhesion testing, *Rev. Sci. Instrum.*, 2007, **78**(7), 072213.

9 L. L. Zhai, G. P. Ling and Y. W. Wang, Effect of nano-Al_2O_3 on adhesion strength of epoxy adhesive and steel, *Int. J. Adhes. Adhes.*, 2008, **28**(1), 23–28.

10 American Society for Testing and Materials, Standard Test Method for Pull-Off Strength of Coatings Using Portable Adhesion Testers, 2017, Report No.: D4541-17, available from: https://www.astm.org/d4541-17.html.

11 S. Pruksawan, G. Lambard, S. Samitsu, K. Sodeyama and M. Naito, Prediction and optimization of epoxy adhesive strength from a small dataset through active learning, *Sci. Technol. Adv. Mater.*, 2019, **20**(1), 1010–1021.

12 L. Cao, D. Russo, K. Felton, D. Salley, A. Sharma, G. Keenan, *et al.*, Optimization of Formulations Using Robotic Experiments Driven by Machine Learning DoE, *Cell Rep. Phys. Sci.*, 2021, **2**(1), 100295.

13 T. Erps, M. Foshey, M. K. Luković, W. Shou, H. H. Goetzke and H. Dietsch, *et al.*, Accelerated Discovery of 3D Printing Materials Using Data-Driven Multi-Objective Optimization, arXiv [cond-mat.mtrl-sci], 2021, available from: http://arxiv.org/abs/2106.15697.

14 Defelsko Corporation, Dolly Preparation for Pull-Off Adhesion Testing, available from: https://www.defelsko.com/resources/dolly-preparation-for-pull-off-adhesion-testing.

15 B. P. MacLeod, F. G. L. Parlane, T. D. Morrissey, F. Häse, L. M. Roch, K. E. Dettelbach, *et al.*, Self-driving laboratory for accelerated discovery of thin-film materials, *Sci. Adv.*, 2020, **6**(20), eaaz8867.

16 B. P. MacLeod, F. G. L. Parlane, C. C. Rupnow, K. E. Dettelbach, M. S. Elliott, T. D. Morrissey, *et al.*, A self-driving laboratory advances the Pareto front for material properties, *Nat. Commun.*, 2022, **13**(1), 1–10.

17 3M, Scotch Weld Epoxy Adhesive DP420 Black DP420 NS Black DP420 Off-White DP420 LH Technical Data, available from: https://multimedia.3m.com/mws/media/1235389O/dp420-technical-data-sheet.pdf.

18 E. Bakshy, L. Dworkin, B. Karrer, K. Kashin, B. Letham and A. Murthy, *et al.*, AE: a domain-agnostic platform for adaptive experimentation, in *Workshop on Systems for ML and Open Source Software at NeurIPS 2018*, 2018, available from: **http://learningsys.org/nips18/assets/papers/87CameraReadySubmissionAE%20-%20NeurIPS%202018.pdf**.

19 B. Letham, B. Karrer, G. Ottoni and E. Bakshy, Constrained Bayesian Optimization with Noisy Experiments, arXiv [stat.ML], 2017, available from: **http://arxiv.org/abs/1706.07094**.

20 N. Taherimakhsousi, B. P. MacLeod, F. G. L. Parlane, T. D. Morrissey, E. P. Booker, K. E. Dettelbach, *et al.*, Quantifying defects in thin films using machine vision, *npj Comput. Mater.*, 2020, **6**(1), 1–6.

21 O. Büyüköztürk, M. J. Buehler, D. Lau and C. Tuakta, Structural solution using molecular dynamics: fundamentals and a case study of epoxy-silica interface, *Int. J. Solids Struct.*, 2011, **48**(14), 2131–2140.

22 S. Sun, A. Tiihonen, F. Oviedo, Z. Liu, J. Thapa, Y. Zhao, *et al.*, A data fusion approach to optimize compositional stability of halide perovskites, *Matter*, 2021, **4**(4), 1092–1094.

23 A. E. Gongora, K. L. Snapp, E. Whiting, P. Riley, K. G. Reyes, E. F. Morgan, *et al.*, Using simulation to accelerate autonomous experimentation: a case study using mechanics, *iScience*, 2021, **24**(4), 102262.

24 B. P. MacLeod, F. G. L. Parlane, A. K. Brown, J. E. Hein and C. P. Berlinguette, Flexible automation accelerates materials discovery, *Nat. Mater.*, 2021, DOI: **10.1038/s41563-021-01156-3**.